

## Photodetachment Spectroscopy of a Doubly Charged Anion: Direct Observation of the Repulsive Coulomb Barrier

Xue-Bin Wang, Chuan-Fan Ding, and Lai-Sheng Wang\*

*Department of Physics, Washington State University, Richland, Washington 99352  
and W. R. Wiley Environmental Molecular Sciences Laboratory, Pacific Northwest National Laboratory,  
MS K8-88, P.O. Box 999, Richland, Washington 99352  
(Received 6 April 1998)*

Photoelectron spectra of citric acid doubly charged anion were measured. The repulsive Coulomb barrier due to the two excess charges was directly probed and estimated to be about  $\sim 1.9$ – $2.5$  eV. The adiabatic binding energy of the second electron was measured to be 1.0 eV. Two detachment channels were observed, with the second channel at  $\sim 0.6$  eV higher in binding energy. The current study presents the first photodetachment experiments of a multiply charged anion and opens up new opportunities to study these novel molecular species. [S0031-9007(98)07383-9]

PACS numbers: 33.80.Eh, 36.90.+f

We report the first photodetachment experiments of a doubly charged anion, citric acid dianion  $[\text{CA}^{2-}, ^- \text{O}_2\text{C}-\text{CH}_2-\text{C}(\text{OH})(\text{CO}_2\text{H})-\text{CH}_2-\text{CO}_2^-]$ ; see Fig. 1(a)]. The experiments were performed with a new apparatus, which couples an electrospray ionization (ESI) source and a magnetic-bottle time-of-flight (TOF) photoelectron analyzer. The photoelectron spectra of  $\text{CA}^{2-}$  were measured at three photon energies: 4.66, 3.49, and 2.33 eV (Fig. 2). An expected long range repulsive Coulomb barrier was observed for the detachment of the doubly charged anion and was estimated to be in the range of  $\sim 1.9$ – $2.5$  eV. An excited state of the  $\text{CA}^-$  singly charged anion was observed in the 4.66 eV detachment spectrum at  $\sim 0.6$  eV above the  $\text{CA}^-$  ground state. The 3.49 eV photon could not access this excited state due to the Coulomb barrier, even though this photon energy was higher than the binding energy of this state. The current experiments represent the first direct observation of the long range Coulomb repulsion barrier in multiply charged anions and demonstrate that photodetachment is a powerful technique to study multiply charged negative ions in the gas phase.

Multiply charged anions are commonly found in the condensed phases. However, few of them are known in the isolated states [1–4], partly due to the fact that many multiply charged anions acquire their stability in the condensed phases through solvation and other electrostatic interactions and are not stable against autodetachment in the gas phase. Even for those multiply charged anions that are stable in the isolated form, the long range Coulomb repulsion between the excess charges makes it difficult for them to be formed in the gas phase [5,6]. Figure 1(b) shows a schematic potential diagram for a doubly charged anion ( $\text{AB}^{2-}$ ) illustrating the repulsive Coulomb barrier (RCB) and the binding energy of the second electron [ $E_b(2)$ ]. The RCB derives from the long range Coulomb repulsion and the short range binding of the excess electron by the singly charged molecule  $\text{AB}^-$ . The potential minimum corresponds to the equilibrium distance between the two

excess electrons in the  $\text{AB}^{2-}$  dianion. In the present case of  $\text{CA}^{2-}$ , this potential minimum corresponds approximately to the distance between the terminal oxygen atoms ( $\sim 6.14$  Å), where the excess charges are localized, as schematically shown in Fig. 1(a). A sufficient separation between the excess charges is necessary for the dianion to be stable. For example, there has been no definitive evidence to show that a single atom can support a stable

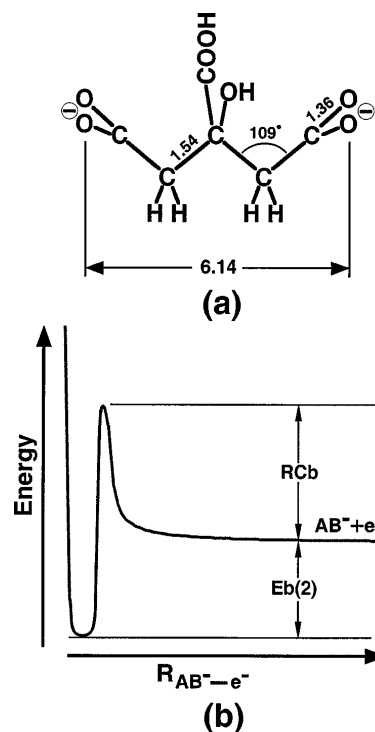


FIG. 1. (a) Schematic structure of the citrate acid dianion with relevant bond length (Å) and bond angle values. (b) Schematic potential energy curve for a doubly charged anion ( $\text{AB}^{2-}$ ) along the electron detachment coordinate.  $E_b(2)$  represents the binding energy of the second excess electron; RCB indicates the repulsive Coulomb barrier experienced by the excess charge.

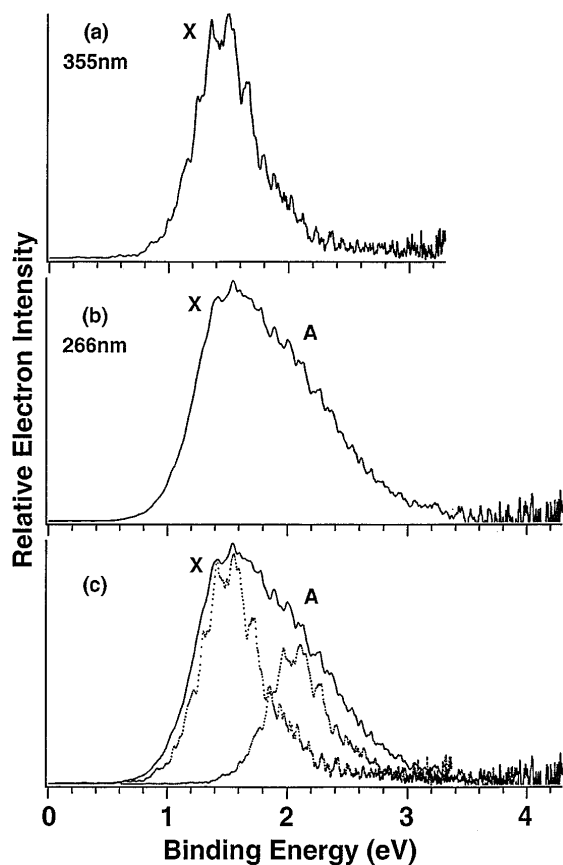


FIG. 2. Photoelectron spectra of citrate acid dianion  $CA^{2-}$  at (a) 355 nm (3.49 eV) and (b) 266 nm (4.66 eV). Note the increased spectral width in the 266 nm spectrum, implying an additional detachment channel as shown in (c) (see text).

dianion due to its small volume [7]. The smallest dianion observed experimentally so far was  $C_7^{2-}$  [8]. Experimental investigation of multiply charged anions heretofore has involved only mass spectrometric techniques [1–4,9]. Several recent works of doubly charged anions have been concerned with carbon clusters and fullerenes [5–8, 10–12]. In particular, Jin *et al.* carried out a series of charge exchange experiments between  $C_{60}F_{48}^{2-}$  and various reagents whose electron affinities were known to be higher than the second electron binding energy of  $C_{60}F_{48}^{2-}$  [11]. The inability to observe any appreciable charge exchange reactions was attributed to a Coulomb barrier. Experimental evidence of RCB in a doubly charged anion has also been reported in a recent experiment involving sequential electron attachment to  $C_{84}^-$  and the subsequent autodetachment of  $C_{84}^{2-}$  [5].

The experiments reported here were performed with a newly developed magnetic-bottle TOF photoelectron spectroscopy apparatus [13,14], interfaced with an ESI source. Recently, it has been shown that the ESI technique [15], which is one of the most powerful means to ionize non-volatile macromolecules in biological mass spectrometry [16], can easily produce gas phase multiply charged anions

that are common in solutions [9,17]. We used a  $10^{-4}$  molar citrate solution at  $pH \sim 10$  in a water/methanol mixed solvent (2/98 ratio) and sprayed it through a 0.01 mm-diam syringe needle at  $-2.2$  kV bias. The highly negatively charged droplets then entered a desolvation capillary (0.8 mm-diam,  $\sim 80^\circ C$ ), which converts the ionic species in the droplet into molecular ions [15]. The anions were then guided by a rf-only quadrupole mass filter into a quadrupole ion trap [18], where they were accumulated for about 0.1 sec before being pushed into the extraction zone of a TOF mass spectrometer (mass resolution,  $M/\Delta M \sim 700$ ). The dominating anion species derived from the citrate solution were  $CA^{2-}$  and  $HCA^-$ . The dianion nature of  $CA^{2-}$  was confirmed by the half mass/charge isotope peaks in the TOF mass spectrum. The  $CA^{2-}$  anions were mass selected and decelerated before being intercepted by a laser beam from a Nd:YAG laser (532, 355, and 266 nm, 7 ns pulse width [19]) in the detachment zone of the magnetic-bottle photoelectron analyzer. Photoelectron TOF spectra were measured and then converted to kinetic energy spectra, calibrated by the known spectra of  $I^-$ ,  $ClO_2^-$ , and  $O^-$  [20]. The energy resolution was about 20 meV FWHM at 0.4 eV kinetic energy, as measured from the spectrum of  $I^-$  at 355 nm and would deteriorate at higher kinetic energies.

The photoelectron spectra of  $CA^{2-}$  are shown in Figs. 2(a) and 2(b) at 355 and 266 nm, respectively. The 355 nm spectrum shows a broad detachment feature with an onset at  $\sim 1.0$  eV, which defines the adiabatic binding energy of the second excess electron  $E_b(2)$  [Fig. 1(b)]. Vibrational structures are discernible, but cannot be assigned to a single progression, indicating that more than one vibrational mode was probably active. The vertical detachment energy was measured to be  $\sim 1.5$  eV. The low energy tail was likely due to hot band transitions. The temperature of  $CA^{2-}$  was expected to be near or slightly above room temperature under our experimental conditions. We also tried to take the photoelectron spectrum of  $CA^{2-}$  at 532 nm (2.33 eV), attempting to improve the spectral resolution. However, no photodetachment signal was observed even though the 532 nm photon energy was higher than the binding energy of the spectral feature [Fig. 2(a)].

The 266 nm spectrum [Fig. 2(b)] appeared quite unusual, compared to the 355 nm spectrum. It is considerably broader at the high binding energy side, suggesting that there might be new detachment channels at the higher photon energy. In Fig. 2(c), the 355 nm spectrum (dotted curve) is overlaid onto the 266 nm spectrum, and the high binding energy feature is clearly revealed. Another copy of the 355 nm spectrum, shifted by 0.6 eV to higher binding energy and at a reduced intensity, is also plotted in Fig. 2(c) to simulate the additional detachment feature. Although the latter procedure is rather crude, it clearly illustrates the existence of an additional detachment feature in the 266 nm spectrum. The two detachment features are

labeled as *X* and *A* in Fig. 2 for the low and high binding energy features, respectively. The shifted 355 nm spectrum is seen to fit the *A* feature rather well, despite the crude nature of the fitting procedure, even the vibrational structures of the *A* feature appear to be similar to the *X* feature of the 355 nm spectrum, suggesting that the *A* and *X* detachment features have very similar Franck-Condon envelopes.

The observation that no detachment took place at 532 nm provided the first evidence for the existence of a RCB [Fig. 1(b)]: even though the 2.33 eV photon energy was higher than the electron binding energy, it was lower than the RCB. Therefore, no detachment could take place except tunneling, which was expected to have very small probability depending on the barrier height and width. From the observations at both 532 and 355 nm, we can conclude that the potential well depth (WD) [see Fig. 1(b)] must be:  $2.33 < \text{WD} < 3.49$  eV, or  $1.33 < \text{RCB} < 2.49$  eV [WD minus the 1.0 eV electron binding energy,  $E_b(2)$ ]. The 266 nm spectrum [Fig. 2(b)] suggested that the well depth involved in the detachment channel leading to the *A* feature was even deeper. The fact that the *A* feature was missing from the 355 nm spectrum offered further evidence for the existence of RCB, in this case for the *A* state, because this photon energy was higher than the binding energy of the *A* state. With this observation, we can derive the WD and RCB for the *A* state to be  $3.49 < \text{WD} < 4.66$  eV, or  $1.89 < \text{RCB} < 3.06$  eV (WD minus the 1.6 eV electron binding energy for the *A* state) [Fig. 3(a)].

The *X* feature represents the transition from the ground state of  $\text{CA}^{2-}$  to that of the radical anion  $\text{CA}^-$ , whereas the *A* feature corresponds to the transition to an electronic excited state of  $\text{CA}^-$ . If we assume that the RCB of both the *X* and *A* states are similar, we can further narrow the range of the RCB down to  $1.89 < \text{RCB} < 2.49$  eV, based on the results presented above. If we use the equilibrium distance between the O atoms on the two  $-\text{CO}_2^-$  groups [6.14 Å, Fig. 1(a)] as the average distance between the two excess charges, we obtain a Coulomb repulsion energy of 2.36 eV [ $e^2/6.14$  (Å)], in remarkable agreement with the RCB value derived experimentally above. The potential energy curves for the *X* and *A* states along the detachment coordinate and the relative energies involved are schematically shown in Fig. 3(a).

The binding energies for the *X* and *A* states and the Coulomb barrier shown in Fig. 3(a) are all relative to the ground vibrational levels of the *X* and *A* states. The photoelectron spectra of  $\text{CA}^{2-}$  shown in Fig. 2 indicate that both the *X* and *A* states contain highly vibrationally excited states with a Franck-Condon envelope of about 1 eV wide for both the *X* and *A* states. For each vibrational level, there should exist a potential curve similar to that shown in Fig. 3(a) for the *X* and *A* states, respectively. Our derived RCB value (between 1.9 and 2.5 eV) and the observation of the broad Franck-Condon envelopes

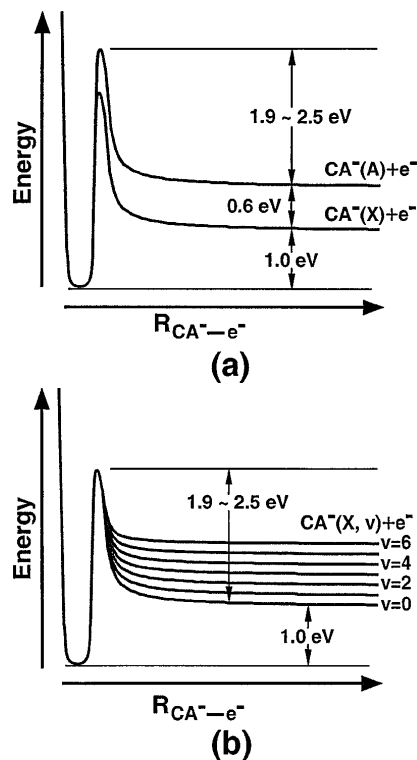


FIG. 3. (a) Schematic potential energy curves showing the adiabatic binding energies and the repulsive Coulomb barrier for detachment of  $\text{CA}^{2-}$ , leading to the *X* and *A* states of  $\text{CA}^-$ . Note that the barrier heights relative to the *X* and *A* states are assumed to be the same. (b) Schematic potential energy curves showing that the repulsive Coulomb barrier decreases for the vibrationally excited levels of  $\text{CA}^-$ .

require that the well depths for both the *X* and *A* states should be relatively invariant with respect to the different vibrational levels, suggesting lower Coulomb barriers for the highly vibrationally excited states of  $\text{CA}^-$ , as shown schematically in Fig. 3(b) for the *X* state.

In photoionization of neutral species or photodetachment of singly charged anions, the long range interaction between the molecular species and the departing electron is attractive. Photodetachment of multiply charged anions provides a unique situation of long range repulsive interaction for the departing electron. Interestingly, the Coulomb repulsion experienced by the detached electron in a multiply charged anion is analogous to the potential felt by a departing  $\alpha$  particle in a radioactive atomic nucleus [1,2,21], even though the length and energy scales are much different in the two cases. Therefore, it would be interesting to understand in detail the potential shape shown in Fig. 1(b) for a multiply charged anion. The barrier height can be measured accurately with a tunable laser. Interesting dynamic effects, tunneling, and barrier reflection would be expected near the top of the potential barrier.

In conclusion, we presented the first photodetachment experiments and photoelectron spectra of a doubly charged anion. The electron binding energy of the second excess

electron in  $CA^{2-}$  or the electron affinity of the  $CA^-$  singly charged radical anion was measured to be about 1.0 eV. The repulsive Coulomb barrier experienced by the excess charges was probed directly and estimated to be between 1.9 and 2.5 eV. A second detachment channel, corresponding to an excited state of  $CA^-$ , was also observed at about 1.6 eV binding energy or 0.6 eV above the ground state of  $CA^-$ . We further deduced that the effective Coulomb barrier decreases for highly vibrationally excited levels of the singly charged anion. The current study demonstrates that photodetachment is a powerful technique to probe the electrostatic interactions and spectroscopy of multiply charged negative ions. It can also be used to investigate the dynamics, solvation effects, and thermochemistry of multiply charged anions in the gas phase.

We are grateful to Dr. Steve Barlow, Dr. Steve Hofstедler, and Dr. L. Pasa-Tolic for their invaluable help and discussion on the quadruple ion guide and trap and electrospray techniques. We also thank Dr. John Price, Dr. Steve Colson, and Dr. Jeff Mack for invaluable discussions and help. This work is supported by the U.S. Department of Energy, Office of Basic Energy Sciences, Chemical Sciences Division and is conducted at the Pacific Northwest National Laboratory, operated for the U.S. Department of Energy by Battelle under Contract No. DE-AC06-76RLO 1830. L. S. W. thanks the Alfred P. Sloan Foundation for their support.

---

\*Author to whom correspondence should be addressed.

- [1] M. K. Scheller, R. N. Compton, and L. S. Cederbaum, *Science* **270**, 1160 (1995).
- [2] R. N. Compton, in *Photophysics and Photochemistry in the Vacuum Ultraviolet*, edited by S. P. McGlynn *et al.* (Reidal, Dordrecht, 1985); in "Negative Ions," edited by V. Esaulov (Cambridge University Press, Cambridge, to be published).
- [3] G. R. Freeman and N. H. March, *J. Phys. Chem.* **100**, 4331 (1996).
- [4] J. Kalcher and A. F. Sax, *Chem. Rev.* **94**, 2291 (1994); A. I. Boldyrev, M. Gutowski, and J. Simons, *Acc. Chem. Res.* **29**, 497 (1996).
- [5] R. N. Compton *et al.*, *Phys. Rev. Lett.* **78**, 4367 (1997).
- [6] O. V. Boltalina *et al.*, *Phys. Rev. Lett.* **80**, 5101 (1998).
- [7] R. N. Compton, in "Negative Ions" (Ref. [2]).
- [8] S. N. Schauer, P. Williams, and R. N. Compton, *Phys. Rev. Lett.* **65**, 625 (1990).
- [9] A. T. Blades and P. Kebarle, *J. Am. Chem. Soc.* **116**, 10761 (1994); A. T. Blades, J. S. Klassen, and P. Kebarle, *ibid.* **117**, 10563 (1995); A. T. Blades, Y. Ho, and P. Kebarle, *J. Phys. Chem.* **100**, 2443 (1996).
- [10] R. L. Hettich, R. N. Compton, and R. H. Rotchie, *Phys. Rev. Lett.* **67**, 1242 (1991); P. A. Limbach *et al.*, *J. Am. Chem. Soc.* **113**, 6795 (1991); G. Khairallah and J. B. Peel, *J. Phys. Chem. A* **101**, 6770 (1997).
- [11] C. Jin *et al.*, *Phys. Rev. Lett.* **73**, 2821 (1994).
- [12] D. Calabrese *et al.*, *J. Chem. Phys.* **105**, 2936 (1996); D. Mathur *et al.*, *Chem. Phys. Lett.* **277**, 558 (1997).
- [13] P. Kruit and F. H. Read, *J. Phys. E* **16**, 313 (1983); O. Cheshnovsky *et al.*, *Rev. Sci. Instrum.* **58**, 2131 (1987).
- [14] L. S. Wang, H. S. Cheng, and J. Fan, *J. Chem. Phys.* **102**, 9480 (1995); L. S. Wang and H. Wu, in *Advances in Metal and Semiconductor Clusters*, edited by M. A. Duncan (JAI Press, Greenwich, 1998), Vol. 4, pp. 299–343.
- [15] M. Yamashita and J. B. Fenn, *J. Phys. Chem.* **88**, 4451 (1984); J. B. Fenn *et al.*, *Science* **246**, 64 (1989).
- [16] *Biochemical and Biotechnological Applications of Electrospray Ionization Mass Spectrometry*, edited by A. P. Snyder (ACS, Washington, DC, 1995).
- [17] T. C. Lau *et al.*, *J. Chem. Soc. Chem. Commun.* **1994**, 1487 (1994); **1995**, 877 (1995).
- [18] *Practical Aspects of Ion Trap Mass Spectrometry*, edited by R. E. March and J. F. J. Todd (CRC Press, New York, 1995), Vols. I–III.
- [19] A range of laser fluences, from 0.05 to 10 mJ/pulse with a 3-mm diam spot size, was used to ensure that there were no multiphoton processes.
- [20] H. Hotop and W. C. Lineberger, *J. Phys. Chem. Ref. Data* **14**, 731 (1985); M. K. Gilles, M. L. Polak, and W. C. Lineberger, *J. Chem. Phys.* **96**, 8012 (1992).
- [21] See, for example, R. Eisberg and R. Resnick, *Quantum Physics of Atoms, Molecules, Solids, Nuclei, and Particles* (Wiley, New York, 1985), 2nd ed.